

Noncommutative geometry of random surfaces

Andrei Okounkov

1 Introduction

1.1

This paper is about a certain interaction between probability and geometry. The random objects involved will be random stepped surfaces spanning a given boundary in \mathbb{R}^3 . Equivalently, one can talk about random rhombi tiling of a planar domain or random dimer coverings of certain subgraphs of the hexagonal graph. Probabilistic questions about these random surfaces will be answered in terms of a nonrandom algebraic object, geometrically a curve in a noncommutative plane.

Underlying this connection is Kasteleyn's theory of planar dimers which computes all probabilities in terms of the Green's function of a certain finite-difference operator K . It will be clear from our construction that the connection between finite-difference operators and noncommutative geometry may be easily extended far beyond what we do in this paper. Our goal here, however, is to explain a certain phenomenon in the least possible generality and to stay as close as possible to certain specific applications. These applications, as well as some other directions that look promising will be discussed below.

1.2

Let Ω be a simply-connected planar domain that can be tiled by rhombi as shown in Figure 1. Well-known bijections illustrated in Figure 1 identify such tilings with dimer coverings of subgraph $\Omega_6 = \Omega \cap \Gamma_6$ of the hexagonal graph Γ_6 and also with *stepped surfaces* spanning given boundary. An introduction to dimers and stepped surfaces may be found in [8].

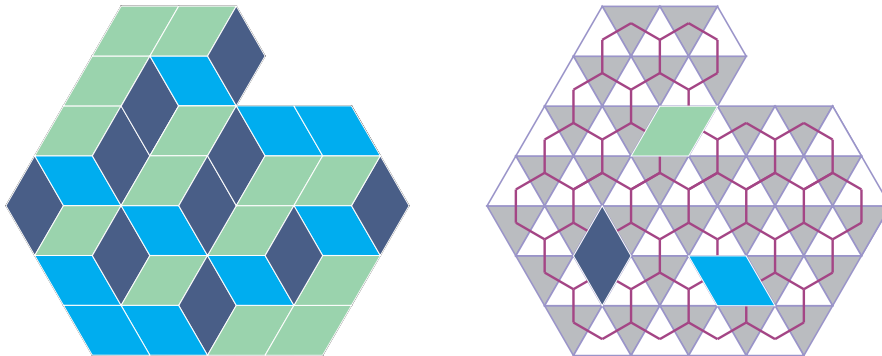


Figure 1: Stepped surfaces are the same as tilings of a planar domain Ω by rhombi. Each tile is a union of a black and white triangle. The adjacency graph of the triangles is (a piece of) the 6-gonal graph.

Stepped surfaces arise in mathematical physics in a variety of contexts: from simply-minded, but realistic models of interfaces (e.g. crystalline surfaces) to the sophisticated setting of super-symmetric gauge and string theories (see e.g. [14, 16] for an introduction).

In all applications, it is natural to weight the probability of a stepped surface S by the volume $V(S)$ enclosed by it, i.e. to set

$$\text{Prob}(S) \propto q^{V(S)}, \quad (1)$$

where $q > 0$ is a parameter. Note that for two surfaces S_1 and S_2 spanning the same boundary the difference $V(S_1) - V(S_2)$ is well-defined, which is all that matters in (1). In the crystal surface context, $\log q$ is the energy price for removing an atom¹

1.3

We will be particularly interested in the case when Ω grows to infinity, while keeping its shape, that is, the number and orientation of its boundary segments. We will refer to such domains as *polygonal*. The study of a random stepped surface a large polygonal boundary (equivalently, random dimer covering, or random tiling) leads to interesting probabilistic questions. The nontriviality of these questions may be appreciated by looking at Figure 2.

¹Note that there is a well-known ambiguity in reconstructing 3-dimensional surfaces

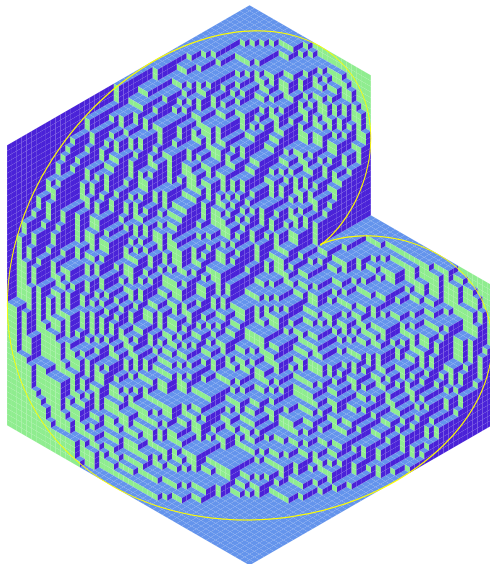


Figure 2: A simulation of the limit shape formation. The curve separating the ordered regions (facets) from the disorder is called the *frozen boundary*. Here, it is a cardioid, i.e. the dual of a rational cubic.

Apparent in Figure 2 is a formation of a certain nonrandom *limit shape*, in other words, as the mesh size goes to zero so does the scale of randomness. This is a form of the law of large numbers. The existence of a limit shape was proven for stepped surfaces (with arbitrary boundary conditions) by H. Cohn, R. Kenyon, and J. Propp in [4].

In [9], the limit shape for polygonal boundaries was linked to a certain plane algebraic curve Q . In particular, the frozen boundary, which is the curve separating order from disorder in Figure 2, is the planar dual of Q in exponential coordinates.

1.4

The main object of this paper may be characterized, informally, as a *quantization* of the limit shape, or of the curve Q to be more specific. This quantization exists for finite Ω , that is, before any limits are taken. In particular, it captures not just the limit shape but also the *fluctuations* of our random

from tiling, namely, one can switch the roles of convex and concave corners. A rotation by $\pi/3$ interchanges the choices. Our conventions are fixed by (2).

surfaces. Viewed like this, it should not be surprising to see noncommutative curves appear. Note, however, that technically the noncommutativity will be linked to the parameter $\log q$ and not to the size of fluctuations (as could be expected from the uncertainty principle).

1.5

In principle, classical Kasteleyn's theory [6] answers all possible questions about random stepped surfaces in terms of the Green's function, i.e. the inverse of a certain difference operator. This *Kasteleyn operator* \mathbf{K} is a weighted adjacency matrix of the graph Ω_6 .

Note that Γ_6 , and hence, Ω_6 is bipartite, that is, its vertices may be colored in two colors (black and white, traditionally) so that only vertices of opposite color are joined by an edge. This is reflected in Figure 3. We will index the rows (resp. columns) of the adjacency matrix by white (resp. black) vertices. The nonzero matrix elements K_{ij} should satisfy

$$q K_{21} K_{43} K_{65} = K_{23} K_{45} K_{61} \quad (2)$$

for each face F , where v_1, \dots, v_6 are the six vertices going around F as in Figure 3. This fixes \mathbf{K} uniquely up to a certain gauge transformation, namely left and right multiplication by a diagonal matrix.

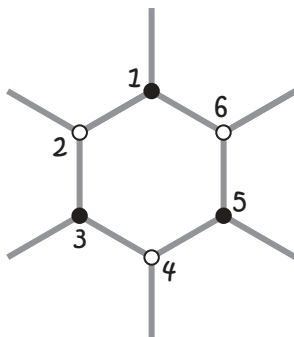


Figure 3: Each hexagon face carries $\log q$ units of magnetic flux.

The goal of this paper may be informally described as looking for some hidden structures in the inverse matrix \mathbf{K}^{-1} . Certain structures in \mathbf{K}^{-1} are plain to see: by definition, the entries of \mathbf{K}^{-1} satisfy a finite-difference equation in each index, namely $\mathbf{K} \mathbf{K}^{-1} = \mathbf{K}^{-1} \mathbf{K} = 1$.

Our main claim is that for polygonal domains Ω the entries of K^{-1} satisfy *additional* finite-difference equations. The degree of these additional equations is determined by the shape of Ω , that is, by the number of boundary segments, and not by the size of Ω . This is crucial from the probabilistic viewpoint.

1.6

The noncommutative geometry of the title provides a natural language to state and study these additional equations.

The origin of the noncommutativity may be traced to (2). For $q = 1$, the adjacency matrix of Γ_6 is an obvious solution and this solution is translation-invariant, i.e. commutes with the subgroup $\mathbb{Z}^2 \subset \text{Aut}(\Gamma_6)$ acting by (bipartition-preserving) translations.

For $q \neq 1$, the translation-invariant equation (2) has no translation-invariant solutions, which means that the Kasteleyn operator K now commutes with *magnetic translations*, i.e. translations followed by a gauge transformation. In turn, magnetic translations commute only up to a factor (whose logarithm is proportional to the area of the parallelogram spanned by the translation vectors). They form, in other words, an algebra known as the quantum 2-torus.

The considerations so far apply only to the whole 6-gonal graph Γ_6 , that is, in the absence of any boundaries. Somewhat remarkably, however, a certain framework may be established in which the Kasteleyn operator and the commuting magnetic translations act in a way compatible with polygonal boundaries. This involves compactifying the quantum 2-torus to a noncommutative plane, meaning that one introduces a certain graded algebra A , a deformation of the ring of polynomials in x_1, x_2, x_3 , such that the quantum 2-torus is the degree 0 part of $A[(x_1x_2x_3)^{-1}]$.

1.7

For any fixed white vertex $w \in \Omega_6$, the action of magnetic translation on $K^{-1}(\cdot, w)$, that is, on the corresponding column of K^{-1} , yields a graded A -module Q^w . The additional equations satisfied by K^{-1} will be reflected in the fact that Q^w is a *torsion* module.

For different w , the modules Q^w share the same fundamental features. In fact, there is a canonical submodule Q in all of them that depends on Ω only

and captures the essential information.

1.8

The construction of the module \mathbf{Q} and the study of its basic properties will occupy the bulk of the present paper. While the definition of \mathbf{Q} involves nothing beyond elementary combinatorics and linear algebra, we will find the resulting object has a certain depth and complexity.

The degrees of its generators and relations (and hence the degrees of the additional equations satisfied by \mathbf{K}^{-1}) are determined by the combinatorics of the domain Ω only, see Theorem 1. On the other hand, the explicit form of these relations depends of q and the geometry of Ω in a rather intricate fashion.

1.9

This is where a geometric way of thinking about such modules, pioneered by M. Artin and his collaborators, becomes essential (see e.g. [21] for an introduction). While its a matter of definitions to associate to \mathbf{Q} a sheaf on the noncommutative plane, the geometric intuition thus gained is very valuable.

In the first place, this is what allows us to view \mathbf{Q} as a quantization of the limit shape Q . In fact, quantization requires additional degrees of freedom, parametrized by line bundles (and more general rank 1 sheaves) on Q . These may be compared to complex phases in quantum mechanics.

Certain features of Q , such as its points of intersection with the coordinate axes of \mathbf{P}^2 have a direct quantum analog satisfied by \mathbf{Q} , see Section 4. Others (such as the geometric genus) are harder to generalize, see [10].

1.10

Because Ω is a purely combinatorial object, we can modify it by simply moving boundary segments in and out. We prove in Section 5 that these transformations act on \mathbf{Q} by what may be called a noncommutative shift on the Jacobian. In particular, this describes what happens to \mathbf{Q} under rescaling of Ω .

1.11 Acknowledgments

The author's present understanding of the subject took some time to develop and I have a large number of people to thank for stimulating and insightful discussions along the way. In particular, I thank D. Eisenbud, V. Ginzburg, A. J. de Jong, R. Kenyon, I. Krichever, D. Maulik, N. Nekrasov, E. Rains, N. Reshetikhin, and Y. Soibelman. Parts of this work grew into joint research projects [10, 19].

I had an opportunity to lecture on the subject on a number of occasions, in particular during the Aisenstadt lectures at the Université de Montréal, T. Wolff lectures at Caltech, Eilenberg lectures at the Columbia University, and Milliman lectures at the University of Washington. I am very grateful to the participants of these lectures for their involvement and feedback. I very much thank these institutions and the Institut des Hautes Études Scientifiques for their warm hospitality during my work on this paper.

2 The quantum limit shape

2.1

Let A be the algebra generated by x_1, x_2, x_3 subject to the relations

$$x_j x_i = q_{ij} x_i x_j, \quad (3)$$

where $q_{ii} = 1$ and $q_{ij} = q_{ji}^{-1}$. This is a basic example of a noncommutative projective plane \mathbf{P}^2 , see e.g. [21] for an introduction. Adding the inverses x_i^{-1} of the generators, we obtain a larger algebra T known as a noncommutative 3-torus.

Both A and T are graded by the total degree in all three generators. Let T_d , where $d \in \mathbb{Z}$ is arbitrary, be one of the graded components. The monomials

$$x^a = x_1^{a_1} x_2^{a_2} x_3^{a_3} \in T_d,$$

obviously correspond to lattice points $a \in \mathbb{Z}^3$ lying in the plane $a_1 + a_2 + a_3 = d$. Their projection in the $(1, 1, 1)$ direction, that is, their image in $\mathbb{R}^3 / \mathbb{R} \cdot (1, 1, 1) \cong \mathbb{R}^2$ may be identified with the black vertices of Γ_6 . In the same fashion, the monomials in T_{d+1} are put into bijection with the white vertices of Γ_6 . This is illustrated for $d = 4$ in Figure 4.

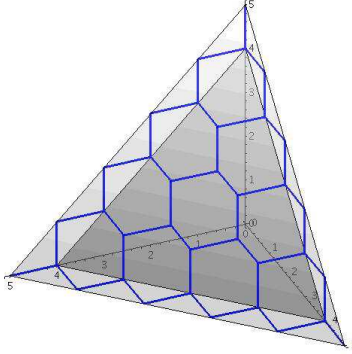


Figure 4: Black and white vertices may be identified with points of \mathbb{Z}^3 lying on two parallel hyperplanes and thus with monomials of two successive degrees. Here we only plot points in $\mathbb{R}_{\geq 0}^3$ which correspond to polynomials in the x_i 's.

2.2

Consider the operator

$$\mathbf{K} : \mathbb{T}_d \rightarrow \mathbb{T}_{d+1}$$

given by right multiplication by $x_1 + x_2 + x_3 \in W_1$, that is,

$$\mathbf{K}f = f \cdot (x_1 + x_2 + x_3).$$

One easily checks from the commutation relations (3) that, indeed, in the basis of monomials, this is a q -weighted Kasteleyn operator for Γ_6 as above, with

$$q = q_{12} q_{23} q_{31}. \quad (4)$$

Note that while there is no canonical ordering of the variables and, hence, no canonical normalization of a monomial, the lines spanned by monomials in \mathbb{T} are well defined. This is all we need since we only care about \mathbf{K} modulo gauge transformations.

2.3 The module M

2.3.1

Monomials are normal in \mathbb{T} , that is, $\mathbf{A}x^c = x^c \mathbf{A}$ is naturally a \mathbf{A} -bimodule. Assuming $\deg x^c \leq 1$, monomials in $(\mathbf{A}x^c)_1$ form a triangle with vertices

$$x_1^{c_1} x_2^{c_2} x_3^{-c_1-c_2+1}, x_1^{c_1} x_2^{-c_1-c_3+1} x_3^{c_3}, x_1^{-c_2-c_3+1} x_2^{c_2} x_3^{c_3} \in \mathbb{T}_1.$$

We denote this equilateral triangle by $\Delta(c)$ and call it the *support* of $(Ax^c)_1$.

2.3.2

We think of black and white vertices in Ω_6 as monomials in \mathbb{T}_0 and \mathbb{T}_1 , respectively. Write Ω as a set-theoretic combination of triangles

$$\Omega = \bigcup_i \Delta(\mathbf{a}_i) \setminus \bigcup_j \Delta(\mathbf{b}_j), \quad \mathbf{a}_i, \mathbf{b}_j \in \mathbb{Z}^3, \quad (5)$$

as in Figure 5. The inclusion of triangles induces the inclusion of graded \mathbb{A} -bimodules

$$\bigoplus \mathbb{A}x^{\mathbf{b}_i} \subset \bigoplus \mathbb{A}x^{\mathbf{a}_i}. \quad (6)$$

We denote by M the quotient \mathbb{A} -bimodule in (6). Define an endomorphism K of M as the right multiplication by $x_1 + x_2 + x_3 \in \mathbb{A}_1$. This is a map of left \mathbb{A} -modules. By construction, the operator

$$K_0 : M_0 \rightarrow M_1$$

is the Kasteleyn operator for Ω_6 .

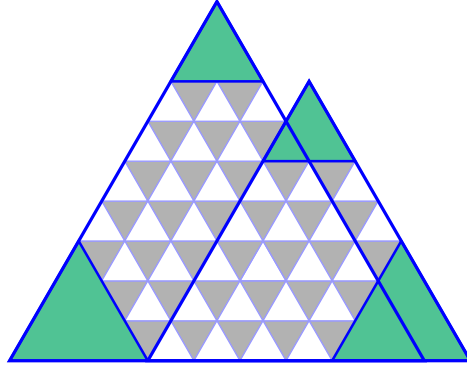


Figure 5: The domain Ω may be represented as a difference of unions of triangles. Here, it is the union of 2 blue triangles minus the union of 4 green ones.

2.3.3

The idea of *stable range* will play an important part in this paper. By definition, a number i is in the stable range for M if the domain

$$\Omega(i) = \text{supp } M_{i+1}$$

has the same combinatorics as $\Omega = \Omega(0)$. In particular, the length of the shortest white boundary of Ω , i.e. a boundary formed by white triangles, gives an upper bound on the stable range.

More generally, refining (5), M may be given a resolution

$$0 \rightarrow F_3 \rightarrow F_2 \rightarrow F_1 \rightarrow F_0 \rightarrow M \rightarrow 0 \quad (7)$$

by modules of the form $\bigoplus \mathbf{A}x^{\mathbf{a}_i}$, where the maps are the natural inclusions. Here $F_0 = \bigoplus \mathbf{A}x^{\mathbf{a}_i}$ corresponds to the triangles $\Delta(\mathbf{a}_i)$ in (5). The intersections among $\mathbf{A}x^{\mathbf{a}_i}$ together with $\Delta(\mathbf{b}_i)$ contribute to relations F_1 , and so on. The module F_0 doesn't have generators of positive degree, but the other F_i 's do. The stable range is until the first such generator appears.

Note that the stable range scales linearly with Ω , meaning that it scales like the inverse mesh size in the probabilistic setup. Throughout the paper, we will only be interested in what happens in the stable range.

2.3.4

Our next goal is to compute the Hilbert function of M_d in the stable range. For that, we will make a genericity assumption that all 3 boundary slopes appear in the boundary $\partial\Omega$ of Ω in a cyclic order. We will denote by $\deg \Omega$ the number of times $\partial\Omega$ cycles through the three slopes. For example, $\deg \Omega = 3$ in Figure 6.

Lemma 1. *For $d \geq 0$ in the stable range, we have*

$$\dim M_d = \dim M_0 - \deg \Omega \frac{d(d-1)}{2} - d \text{ ind } \mathbf{K}_0.$$

Here, of course, the index of \mathbf{K}_0 equals zero, but it will not vanish in the generalizations considered below.

Proof. Consider the map

$$M_d \ni f \mapsto x_3 f \in M_{d+1}. \quad (8)$$

The kernel and cokernel of this map are formed by functions supported on horizontal strips of the form shown in Figure 6. More precisely, white horizontal boundaries correspond to the cokernel, the black ones — to the kernel.

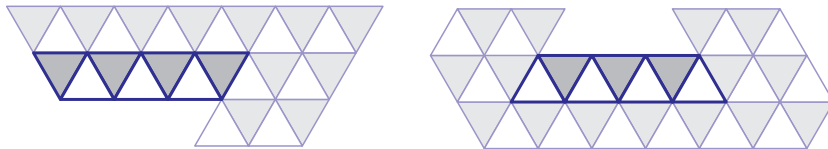


Figure 6: A white (left) and black (right) boundary strips. Note that they always have the same shape provided the boundary of Ω cycles through the 3 directions.

Note that white boundaries of $\text{supp } M_i$ shrink with i , while the black ones expand. Thus each of the $\deg \Omega$ horizontal boundaries contributes -1 to the second derivative of $\dim M_i$ with respect to i . We conclude

$$\dim M_d = -\deg \Omega \frac{d^2}{2} + \dots, .$$

Here dots stand for a polynomial in d of degree ≤ 1 , which is uniquely fixed by its evaluation at $d = 0, 1$. \square

2.3.5

Lemma 2. *The operator $\mathbf{K} : M_d \rightarrow M_{d+1}$ is surjective for $d \geq 0$ in the stable range and $q > 0$ or q generic.*

Proof. For $d = 0$, by Kasteleyn's theorem, $\det \mathbf{K}$ determinant gives the q -weighted count of stepped surfaces, hence nonzero for $q > 0$. For $d > 0$, we use the commuting map (8) and induction. By induction, it suffices to check the surjectivity of \mathbf{K} on a white boundary strip, as in Figure 6, which is immediate. \square

2.4 The module \mathbf{Q} and the inverse Kasteleyn matrix

2.4.1

We denote by \mathbf{Q} the kernel of \mathbf{K} acting on M . This is a graded left \mathbf{A} -module. To see why this may be a useful definition, let us generalize the construction slightly.

2.4.2

Let w be a white vertex of Ω_6 corresponding to a monomial x^w . Let Ω^w be obtained from Ω by removing the corresponding white triangle and set

$$M^w = M / \mathbf{A} x^w.$$

The conclusions of Lemmas 1 and 2 continue to hold for M^w , with the obvious modification that

$$\deg \Omega^w = \deg \Omega + 1, \quad \text{ind } \mathbf{K}_0^w = 1.$$

In contrast to \mathbf{Q} , we have $\mathbf{Q}_0^w \neq 0$. Indeed, by construction, \mathbf{Q}_0^w is spanned by the corresponding column $\mathbf{K}^{-1} x^w$ of the inverse Kasteleyn matrix.

Via the left \mathbf{A} -module structure on \mathbf{Q}^w , the algebra \mathbf{A} acts on the columns of the inverse Kasteleyn matrix by difference operators. To see that a nonzero difference operator from \mathbf{A} must annihilate \mathbf{Q}_0^w , it will suffice to compute the Hilbert function of \mathbf{Q}^w .

2.4.3

From Lemmas 1 and 2 we have, in the stable range,

$$\dim \mathbf{Q}_d = d \deg \Omega + \text{ind } \mathbf{K}_0 = d \deg \Omega \tag{9}$$

and, similarly,

$$\dim \mathbf{Q}_d^w = (\deg \Omega + 1) d + 1. \tag{10}$$

Since these dimensions grow only linearly in d , for any $g \in \mathbf{Q}_d$ the map

$$\mathbf{A}_i \ni f \mapsto f \cdot g \in \mathbf{Q}_{d+i}$$

must have a kernel as soon as i is large enough. These are the sought difference equations satisfied by \mathbf{K}^{-1} . We will, obviously, have to do more work to say something more specific about them.

2.4.4

Note that we have an exact sequence

$$0 \rightarrow \mathbf{Q} \rightarrow \mathbf{Q}^w \rightarrow L \rightarrow 0, \tag{11}$$

where the third term L satisfies $\dim L_d = d + 1$. In fact, L is a *line module*, i.e. the module of the form

$$L = \mathbf{A}/\mathbf{A}l, \quad l \in \mathbf{A}_1.$$

Lemma 3. *In the stable range, i.e. for \mathbf{w} sufficiently far from the boundary of Ω , L is a line module with $l = x^{\mathbf{w}}(x_1 + x_2 + x_3)x^{-\mathbf{w}}$.*

Proof. Let $g = \mathbf{K}^{-1}x^{\mathbf{w}}$ be the generator of $\mathbf{Q}_0^{\mathbf{w}}$ and suppose $fg \in \mathbf{Q}$ for some $f \in \mathbf{A}$. This means that fg may be extended to all of Ω as a solution of Kasteleyn's equation. In other words, there exists a polynomial $g' \in \mathbf{A}_{\deg f - 1}$ such that

$$0 = \mathbf{K}(fg + g'x^{\mathbf{w}}) = fx^{\mathbf{w}} + g'x^{\mathbf{w}}(x_1 + x_2 + x_3),$$

proving the assertion. \square

From this perspective, there isn't much difference between \mathbf{Q} and $\mathbf{Q}^{\mathbf{w}}$.

Somewhat poetically, we will call \mathbf{Q} the *quantum limit shape*. Mathematical reasons for this name will be discussed below.

3 The structure of \mathbf{Q}

3.1

The goal of this Section is to prove the following

Theorem 1. *In the stable range and for generic q , \mathbf{Q} is generated by $\deg \Omega$ generators of degree 1 subject to $\deg \Omega$ linear relations. In other words, the minimal graded free resolution of \mathbf{Q} has the form*

$$0 \rightarrow \mathbf{A}(-2)^{\deg \Omega} \rightarrow \mathbf{A}(-1)^{\deg \Omega} \rightarrow \mathbf{Q} \rightarrow 0. \quad (12)$$

Similarly,

$$0 \rightarrow \mathbf{A}(-2)^{\deg \Omega} \rightarrow \mathbf{A} \oplus \mathbf{A}(-1)^{\deg \Omega - 1} \rightarrow \mathbf{Q}^{\mathbf{w}} \rightarrow 0. \quad (13)$$

Here we denote, as customary, $\mathbf{A}(i)_d = \mathbf{A}_{i+d}$.

3.2

In the commutative case, resolutions of the form (12) are well known in algebraic geometry, see, in particular, [1]. The corresponding sheaves on \mathbf{P}^2 are of the form $\iota_*\mathcal{L}$, where

$$\iota : Q \rightarrow \mathbf{P}^2$$

is an inclusion of a curve of degree $D = \deg \Omega$ and \mathcal{L} is a line bundle \mathcal{L} (or a more general torsion-free sheaf in case Q is singular) of degree $g - 1$. Here

$$g = (D - 1)(D - 2)/2$$

is the arithmetic genus of Q . Concretely,

$$Q = \det R,$$

where R is the matrix of linear forms that gives the map

$$R : \mathbf{A}(-2)^D \rightarrow \mathbf{A}(-1)^D$$

in (12). The condition in (12) on \mathcal{L} to have no sections means $\mathcal{L} \in \text{Jac}_{g-1}(Q) \setminus \Theta$, where $\Theta \subset \text{Jac}_{g-1}(Q)$ is the theta divisor.

The meaning of (13) is parallel, with the difference that D becomes $\deg \Omega + 1$ and $\deg \mathcal{L}$ becomes g . In the commutative case, (11) implies the support of \mathbf{Q}^w has the line $l = 0$ as a component.

3.3

One of the eventual goals of the present project is to understand the behavior of \mathbf{Q} as the mesh size goes to 0 while $\log q \rightarrow 0$ at a comparable rate. The moduli of sheaves of the form (12) have a natural compactification, which guarantees that any sequence has a subsequence converging to an actual sheaf on the usual commutative plane \mathbf{P}^2 .

It will be shown in [10] that this limit is supported on the curve Q corresponding to the limit shape. This is the reason for calling \mathbf{Q} the quantum limit shape.

3.4

For any graded \mathbf{A} -module \mathbf{Q} , the degrees of its generator, relations, etc., may be read off the dimensions of the graded components of the vector spaces

$$\text{Tor}_i \mathbf{Q} = \text{Tor}_i(\mathbf{A}/\mathbf{A}_{>0}, \mathbf{Q}),$$

where $A_{>0}$ is the ideal generated by A_1 . In particular, the existence of a free resolution of length 2 is equivalent to the following

Lemma 4. *In the stable range of degrees, $\text{Tor}_i \mathbf{Q} = 0$ for $i > 1$.*

Proof. Since $\text{Tor}_{>3}$ vanish identically for the algebra \mathbf{A} , we need to show the vanishing for $i = 2, 3$. Since the resolution (7) is defined combinatorially in terms of Ω , we conclude $\text{Tor}_i M = 0$ in the stable range. This is, really, the definition of the stable range. Since $\mathbf{Q} \subset M$ and $\text{Tor}_4 = 0$ identically, we conclude

$$\text{Tor}_3 \mathbf{Q} = 0.$$

By construction, there is an exact sequence

$$0 \rightarrow \mathbf{Q} \rightarrow M \rightarrow \text{Im } \mathbf{K} \rightarrow 0,$$

and since $\text{Im } \mathbf{K} \subset M$, we have $\text{Tor}_3 \text{Im } \mathbf{K} = 0$. Now from the long exact sequence for Tor_i , it follows that $\text{Tor}_2 \mathbf{Q} = 0$. \square

3.5

Lemma 5. *For generic q , \mathbf{Q} is generated by \mathbf{Q}_1 .*

Proof. It suffices to consider the commutative case $q_{ij} = 1$. Then, on the one hand, \mathbf{Q} is annihilated by $x_1 + x_2 + x_3$, while on the other $\text{Tor}_i \mathbf{Q} = 0$, $i > 1$. This means \mathbf{Q} corresponds to a vector bundle on the line $x_1 + x_2 + x_3 = 0$. From its Hilbert polynomial, we see that it must be $\mathcal{O}(-1)^{\text{deg } \Omega}$, whence the conclusion. \square

3.6

Now it is easy to complete the proof of (12). We have $\text{deg } \Omega = \dim \mathbf{Q}_1$ generators in degree 1 and from (9) we see that they must satisfy $\text{deg } \Omega$ linear relations. There are no other generators by Lemma 5 and no other relations by (9).

The proof of (13) goes along the same lines. Lemma 4 still holds even though $(\text{Tor}_1 M^w)_1 \neq 0$. The analog of Lemma 5 is that \mathbf{Q}^w is generated in degrees 0 and 1, because in the commutative case \mathbf{Q} corresponds to the bundle $\mathcal{O} \oplus \mathcal{O}(-1)^{\text{deg } \Omega}$ on the line $x_1 + x_2 + x_3 = 0$.

It remains to explain why the commutative resolution

$$0 \rightarrow \mathbf{A}(-1) \oplus \mathbf{A}(-2)^{\deg \Omega} \rightarrow \mathbf{A} \oplus \mathbf{A}(-1)^{\deg \Omega} \rightarrow \mathbf{Q}^w \rightarrow 0, \quad q_{ij} = 1,$$

jumps to (13) for generic q . In other words, we need to check that the generator of \mathbf{Q}_0^w no longer satisfies a linear relation for generic q . This is an easy consequence of the results of the next section.

Namely, a linear polynomial meets $x_1x_2x_3$ in 3 points, that is, it annihilates 3 generators of point modules over \mathbf{A} . As we will see, the annihilator of \mathbf{Q}_0^w meets each coordinate axis in $\deg \Omega + 1$ points.

4 Boundary points

4.1

Recall from [9] that the curve Q describing the limit shape is determined as the unique rational curve of degree $\deg \Omega$ for which the dual curve Q^\vee is inscribed in Ω . This means, in particular, that Q meets each coordinate line of \mathbf{P}^2 in $\deg \Omega$ specified points.

In this section, we will see that the quantum limit shape \mathbf{Q} satisfies the exact noncommutative analog of this incidence.

4.2

We define

$$\partial_3 \mathbf{Q} = \mathbf{Q} / x_3 \mathbf{Q}.$$

We will see that $\partial_3 \mathbf{Q}$ is a direct sum of $\deg \Omega$ point modules labeled by the horizontal boundaries of Ω as in Figure 6.

By definition, the Hilbert polynomial of a *point module* is equal to the constant 1. Up to modules of finite length, point modules are parametrized by the toric divisor $x_1x_2x_3 = 0$ of \mathbf{P}^2 . The correspondence is as follows

$$(a_1 : a_2 : 0) \leftrightarrow \mathbf{A} / \langle x_3, a_2x_1 - a_1x_2 \rangle.$$

The ratios a_2/a_1 for the summands of $\partial_3 \mathbf{Q}$ will be determined by the vertical coordinate of the horizontal boundaries of Ω .

4.3

The Hilbert function evaluation

$$\dim (\partial_3 \mathbf{Q})_d = \deg \Omega, \quad d > 0,$$

is a consequence of the following

Lemma 6. *Left multiplication by x_3 has no kernel acting on \mathbf{Q} .*

Proof. A polynomial in the kernel of left multiplication by x_1 has a support in a strip of width 1 along the black boundaries, as in Figure 6, right. It is impossible for such function to be annihilated by the Kasteleyn operator. \square

4.4 White boundaries

Let Ω' be a nontileable domain obtained by moving one of the white horizontal boundaries of Ω one step in. Denote by M' the corresponding monomial module. Let $K' : M' \rightarrow M'$ be right multiplication by $x_1 + x_2 + x_3$ and let $Q' = Q \cap M'$ be its kernel. Since $x_3 Q \subset M'$, $\partial_3 Q$ surjects onto Q/Q' .

By cutting white boundary strips off $\Omega'(i)$, $i > 1$, we see as in the proof of Lemma 2 that K' surjects onto M'_i for $i > 1$. Since $\text{ind } K'_0 = -1$, it follows from Lemma 1 that Q/Q' is a point module.

Lemma 7. *Let a be the vertical coordinate of the strip $\Omega \setminus \Omega'$, that is, let $\deg_{x_3} f = a$ for all $f \in M/M'$. Then*

$$Q/Q' \cong \mathbf{A} / \langle x_3, x_1 + q^a x_2 \rangle (1),$$

starting in degree 1.

Proof. The series

$$(x_1 + x_2)^{-1} = x_1^{-1} - x_1^{-1} x_2 x_1^{-1} + x_1^{-1} x_2 x_1^{-1} x_2 x_1^{-1} - \dots$$

gives 1 after left or right multiplication by $(x_1 + x_2)$. Interchanging the roles of x_1 and x_2 and taking the difference

$$\delta = (x_1 + x_2)^{-1} - (x_1 + x_2)^{-1}$$

we get an analog of the usual δ -function, which is annihilated by both left and right multiplication by $(x_1 + x_2)$.

An element of $(\mathbb{Q}/\mathbb{Q}')_d$ is a truncation of the series $x_3^a x_1^{-a+d+1} \delta$ on both sides. Left multiplication by

$$x_1 + q^a q_{21}^{d+1} x_2$$

annihilates it, whence the conclusion. \square

4.5 Black boundaries

Now let Ω' be a nontileable domain obtained by moving one of the black horizontal boundaries of Ω one step out. We have a map $M' \rightarrow M$ corresponding to the restriction of functions and from Lemma 6 we conclude that it yields an injection $\mathbb{Q}' \rightarrow \mathbb{Q}$. Further, $x_3 \mathbb{Q}$ is in the image of \mathbb{Q}' , hence \mathbb{Q}/\mathbb{Q}' is again a point module onto which $\partial_3 \mathbb{Q}$ surjects.

Lemma 8. *Let a be the vertical coordinate of the strip $\Omega' \setminus \Omega$, that is, let $\deg_{x_3} f = a$ for all f in the kernel of the restriction map $M' \rightarrow M$. Then*

$$\mathbb{Q}/\mathbb{Q}' \cong \mathbf{A} / \langle x_3, x_1 + q^a x_2 \rangle (1),$$

starting in degree 1.

Proof. Let f be in \mathbb{Q}_d and denote by $f_{d-a+1} x_3^{a-1}$ the monomials in f along the boundary in question. Here f_{d-a+1} denotes a polynomial in x_1 and x_2 of degree $d-a+1$. Clearly, f may be extended to an element in \mathbb{Q}' if and only if we can find a polynomial $g_{d-a}(x_1, x_2) x_3^a$ with support in $\Omega' \setminus \Omega$ such that

$$f_{d-a+1} x_3^a = g_{d-a} x_3^a (x_1 + x_2).$$

The commutation relations in \mathbf{A} imply that for any $f_k \in \mathbf{A}_k$ which does not depend on x_3 and any C we can find $f'_k \in \mathbf{A}_k$ such that

$$(x_1 + C x_2) f_k = f'_k (x_1 + q_{12}^k C x_2).$$

From this it follows that $x_1 + q^a q_{21}^{d+1} x_2$ annihilates $(\mathbb{Q}/\mathbb{Q}')_d$, as was to be shown. \square

4.6

We can summarize the discussion as follows.

Theorem 2. *We have*

$$\partial_3 \mathbf{Q} \cong \bigoplus_{i=1}^{\deg \Omega} \mathbf{A} / \langle x_3, x_1 + q^{a_i} x_2 \rangle (1), \quad (14)$$

starting in degree 1, where a_i are the heights of the horizontal boundaries of Ω as above.

Proof. The Hilbert polynomial equals the constant $\deg \Omega$ on both sides. We constructed a map from the LHS to the RHS in (14). Its kernel consists of functions f that vanish on the boundary strips along the white boundaries of Ω and may be extended as solutions of $\mathbf{K}f = 0$ to a horizontal strip just beyond the black boundaries of Ω . This modified domain is a translate of $\Omega(-1)$ in the x_3 direction and our conditions on f imply $f \in x_3 \mathbf{Q}$. Thus the map above is an isomorphism. \square

5 Correspondences and renormalization

5.1

Let Ω' be obtained from Ω by moving one boundary segment by one step, as in Sections 4.4 and 4.5. We found that the corresponding modules \mathbf{Q} and \mathbf{Q}' fit into an exact sequence of the form

$$0 \rightarrow \mathbf{Q}' \rightarrow \mathbf{Q} \rightarrow P \rightarrow 0 \quad (15)$$

with a point module P . Modules of the form (12) form an open set in the moduli spaces of \mathbf{A} -modules of rank 0 and

$$(c_1, c_2) = (D, D(D+3)/2), \quad D = \deg \Omega.$$

Let $\mathcal{M}(c_1, c_2)$ denote a finite cover of this open set over which the ordering of the summands in (14) is chosen.

For general c_2 , we define $\mathcal{M}(c_1, c_2)$ as the moduli space of \mathbf{A} -modules with the same minimal resolution as the generic commutative resolution plus an ordering of boundary points. For example, for

$$(c_1, c_2) = (D, D(D+3)/2 - k), \quad 0 \leq k \leq D/2,$$

the corresponding modules \mathbf{Q}'' are of the form

$$0 \rightarrow \mathbf{A}(-2)^{D-k} \rightarrow \mathbf{A}^k \oplus \mathbf{A}(-1)^{D-k} \rightarrow \mathbf{Q}'' \rightarrow 0,$$

generalizing (13).

5.2 Noncommutative shift on the Jacobian

It is easy to see that

$$\dim \mathcal{M}(c_1, c_2) = c_1^2 + 1,$$

and, in particular, it doesn't depend on c_2 .

Lemma 9. *The correspondence*

$$\{(\mathcal{Q}', \mathcal{Q})\} \subset \mathcal{M}(c_1, c_2 + 1) \times \mathcal{M}(c_1, c_2)$$

defined by (15) is the graph of a birational map.

Proof. It suffices to consider the commutative case, when this becomes a shift by P on the Jacobian of the curve Q , see Section 3.2. \square

This means that we have an action of a group $\mathbf{S} \cong \mathbb{Z}^{3c_1}$ on $\bigsqcup_{c_2} \mathcal{M}(c_1, c_2)$ by birational transformations. A subgroup of the form \mathbb{Z}^{3c_1-1} preserves c_2 and acts birationally on individual components. Perhaps the title of this subsection is the appropriate name for this group action.

Parallel group actions may be defined for other noncommutative surfaces. They turn out to encompass several previously studied discrete dynamical systems. This is the subject of a joint work by E. Rains and the author, the results of which will appear in [19].

5.3

Renormalization is a central concept in mathematical physics. For any tileable domain Ω and any $m \in \mathbb{Z}_{>0}$, the scaled domain $m\Omega$ is again tileable and it is natural to ask how this scaling transformation affects our random surfaces. Equivalently, of course, one can keep Ω fixed and divide the mesh size by m .

To quantify the word ‘‘affects’’, one tries to summarize the behavior of random surfaces in terms of finitely many essential degrees of freedom. One further hopes to define an action of the group $\mathbb{R}_{>0}$ on this space extending the scaling transformations above.

While this procedure is a very powerful guiding principle, in practice one usually has to use various approximations to make it work. This is only natural since one is trying to squeeze an infinite-dimensional problem into a finite-dimensional dynamical system.

5.4

Our kind of problems are special in that they have a certain built-in finite-dimensionality, starting from a finite number segments that bound Ω . The quantum limit shape Q also varies in a finite-dimensional moduli space. Since Q encodes the essential information about the correlation functions, the renormalization dynamics may be considered understood once the scaling action on Q is determined.

Clearly, scaling transformations are composed out of many noncommutative shifts on the Jacobian, and more precisely we have

Theorem 3. *The scaling $\Omega \mapsto m \cdot \Omega$ preserves the S -orbit of Q and intertwines the action of $s \in S$ with the action of $m \cdot s \in S$.*

5.5

If the parameter q is adjusted simultaneously, then the limit $m \rightarrow \infty$ becomes the *thermodynamic* limit

$$\text{mesh} \rightarrow 0, \quad \log q = O(\text{mesh}),$$

which is the limit that we were planning to take all along. In this limit, noncommutative shifts of the Jacobian may be viewed as a perturbation of the commutative shift, thus joining a much-studied area of perturbations of integrable systems. Their analysis from this point of view will appear in [10].

In particular, it will be shown in [10] that, indeed the quantum limit shape Q is a deformation of the curve Q that defines the (classical) limit shape.

6 Outlook

6.1

The Kasteleyn operator on Γ_6 has an infinite-dimensional kernel and the Kasteleyn equation needs to be supplemented by boundary conditions in order to have a unique solution. By contrast, once a second difference equation of degree d is known, the solutions form a d -dimensional linear space, spanned by modulated plane waves. This simple principle gives a powerful

way to control K^{-1} in the thermodynamic limit which is the basic analytic issue in the analysis of stepped surfaces.

In fact, optimistically, one may expect these techniques to overcome the difficulties that lie in the way of proving the CLT for stepped surfaces with polygonal boundaries (see [7] for techniques that can handle a different sort of boundary conditions) as well determining the local correlations. Further, since polygonal boundaries are dense in the space of all boundaries, the calculation of local correlations for them has direct implication to the classification of Gibbs measures (about which [20] contains a wealth of information).

6.2

Kasteleyn theory and the formalism of [9] work for any periodic bipartite planar dimer. It would be very interesting to study the quantum limit shape in this generality. It would be also very interesting to find applications to difference equations other than the Kasteleyn equation, such as e.g. discrete Dirac equations in dimensions > 2 .

6.3

For very special kinds of boundary conditions (see e.g. [16, 17] for an introduction) the q -weighted stepped surface partitions functions Z become generating functions Z_{DT} for the Donaldson-Thomas invariants of toric CY three-folds².

Very generally, for any smooth projective three-fold X the expansion of $\log Z_{DT}$ in powers of $\log q$ was conjectured to generate the Gromov-Witten invariants of the same three-fold X , genus by genus [11]. For a toric three-fold X , this conjecture was proven in [12].

In particular, this relates the genus 0 Gromov-Witten invariants of X to the leading asymptotics of $\log Z$ as $\log q \rightarrow 0$, and hence to the limit shape Q . *Mirror symmetry*, which is certainly too complex and multifaceted a phenomenon to be discussed here with any precision, associates basically the same curve Q to X . Thus the limit shape point of view puts mirror symmetry on a firm probabilistic ground in this particular instance.

The quantum limit shape Q captures the fluctuations and hence all orders of the expansion of $\log Z$. This makes it a strong candidate for the as yet

²The customary parameter q in DT theory differs from ours by a minus sign.

mysterious higher-genus mirror of X . Moreover, the quantum limit shape Q , being a categorical object, might stand a better chance of generalization to non-toric X than the underlying box-counting. Progress in this direction remains both very desirable and scarce.

6.4

There exists a different (and, at present, conjectural) way to extract the higher genus GW invariants out of Q , which was proposed in [2] based on the diagrammatic techniques developed in the random matrix context, see in particular [3]. The use of noncommuting variables in a related context was advocated, in particular, in [5].

It is reasonable to expect the two approaches to converge, especially since various random matrix models may naturally be viewed as continuous limits of stepped surfaces. For example, one sees random matrices quite directly near the points where Q intersects the coordinate axes [18]. There are also numerous parallels between random matrices and Plancherel-like measures on partitions, which are induced on slices of stepped surfaces [15].

A more ambitious goal may be to push the theory away from the $K_X = 0$ case. As a first problem in the $K_X \neq 0$ direction, one can try the equivariant vertex [11, 12]. As a random surface model, it is very nonlocal and otherwise distant from what is perceived as natural in statistical mechanics. To its credit, it has a map, due to Nekrasov [13], onto certain local 2-dimensinal lattice fermions. In contrast to Kasteleyn theory, these fermions are now interacting and it remains to be seen how much progress one can make in this more general setting.

References

- [1] A. Beauville, *Determinantal hypersurfaces*, Mich. Math. J. **48**, 39–64 (2000).
- [2] V. Bouchard, A. Klemm, M. Marino, S. Pasquetti, *Remodeling the B-model*, Comm. Math. Phys. 287 (2009), no. 1, 117–178.
- [3] L. Chekhov, B. Eynard, N. Orantin, *Free energy topological expansion for the 2-matrix model*. J. High Energy Phys. 2006, no. 12.

- [4] Cohn, H., Kenyon, R., Propp, J., A variational principle for domino tilings, *Journal of AMS*, **14**(2001), no. 2, 297-346.
- [5] R. Dijkgraaf, L. Hollands, P. Sulkowski, C. Vafa, *Supersymmetric gauge theories, intersecting branes and free fermions*, J. High Energy Phys. 2008, no. 2.
- [6] P. Kasteleyn, *Graph theory and crystal physics*, Graph Theory and Theoretical Physics, 43–110, Academic Press, 1967
- [7] R. Kenyon, *Height fluctuations in honeycomb dimers*, math-ph/0405052.
- [8] R. Kenyon, *Lectures on dimers*, available from <http://www.math.brown.edu/~rkenyon/papers/dimerlecturenotes.pdf>
- [9] R. Kenyon and A. Okounkov, *Limit shapes and complex Burgers equation*, math-ph/0507007.
- [10] I. Krichever and A. Okounkov, in preparation.
- [11] D. Maulik, N. Nekrasov, A. Okounkov, and R. Pandharipande, *Gromov-Witten theory and Donaldson-Thomas theory, I. & II.*, math.AG/0312059, math.AG/0406092.
- [12] D. Maulik, A. Oblomkov, A. Okounkov, and R. Pandharipande, *Gromov-Witten/Donaldson-Thomas correspondence for toric 3-folds*, arXiv:0809.3976.
- [13] N. Nekrasov, *Topological strings and two dimensional electrons*, The Quantum Structure of Space and Time, Proceedings of the 23rd Solvay Conference on Physics, edited by D. Gross, M. Henneaux, A. Sevrin, World Scientific, 2007.
- [14] N. Nekrasov, *Instanton partition functions and M-theory*, Vth Takagi Lectures, Japan. J. Math. 4, 63-93 (2009)
- [15] A. Okounkov, *The uses of random partitions*, XIVth International Congress on Mathematical Physics, 379–403, World Sci., 2005.

- [16] A. Okounkov, *Random surfaces enumerating algebraic curves*, Proceedings of Fourth European Congress of Mathematics, EMS, 751–768, [math-ph/0412008](#).
- [17] A. Okounkov, *Geometry and physics of localization sums*, <http://www.math.columbia.edu/~thaddeus/seattle/okounkov.pdf>.
- [18] A. Okounkov, *The birth of a random matrix*, Mosc. Math. J. **6** (2006), no. 3, 553–566.
- [19] E. Rains and A. Okounkov, in preparation.
- [20] S. Sheffield, *Random surfaces*, Astérisque **304** (2005).
- [21] J. T. Stafford and M. Van den Bergh, *Noncommutative curves and noncommutative surfaces*, Bull. AMS **38** (2001), 171–216.